Available online at www.sciencedirect.com
ScienceDirect
Journal of Hazardous Materials 152 (2008) 347–355
Journal of Hazardous Materials
www.elsevier.com/locate/jhazmat

TiO_2 hydrosols with high activity for photocatalytic degradation of formaldehyde in a gaseous phase

Tong-xu Liu [a,d], Fang-bai Li [b,*], Xiang-zhong Li [c]

[a] *Guangzhou Institute of Geochemistry, Chinese Academy of Sciences, Guangzhou 510640, PR China*
[b] *Guangdong Key Laboratory of Agricultural Environment Pollution Integrated Control, Guangdong Institute of Eco-Environment and Soil Science, Guangzhou 510650, PR China*
[c] *Department of Civil and Structural Engineering, The Hong Kong Polytechnic University, Kowloon, Hong Kong, PR China*
[d] *Graduate School of the Chinese Academy of Sciences, Beijing 100039, PR China*

Received 14 March 2007; received in revised form 2 July 2007; accepted 3 July 2007
Available online 7 July 2007

Abstract

Two types of TiO_2 hydrosols (TOSO and HTO) were prepared from titanium sulfate ($TiOSO_4$) and metatitanic acid (H_2TiO_3) by a chemical precipitation–peptization method, respectively. The prepared hydrosols were characterized by means of X-ray diffraction, particle size distribution, scanning electron microscopy, UV–vis spectroscopy, Fourier transform infrared spectroscopy, Brunauer–Emmett–Teller and Barret–Joyner–Halender methods. The results showed that the TiO_2 hydrosols with an anatase crystal structure had smaller particle sizes, higher surface areas, larger pore volume, and higher transparence than Degussa P-25 suspension. The photocatalytic activity of the TiO_2 hydrosols was evaluated for formaldehyde degradation under UVA illumination in a gaseous phase. The results demonstrated that the photocatalytic activity with the catalyst loading of 2 mg cm^{-2} was ranked as an order of HTO > TOSO > P-25. The photocatalytic activity was further studied using the HTO catalyst under different experimental conditions. The results showed that catalyst loading, relative humidity, and initial concentration could influence the efficiency of HCHO photocatalytic degradation. It was found that a catalyst loading of more than 2 mg cm^{-2} and a relative humidity of 55% were two essential conditions for achieving the best performance under these experimental conditions. The repeated experiments indicated that the HTO catalyst was reasonably stable and could be repeatedly used for the HCHO oxidation under UVA irradiation. This investigation would be helpful to promote the application of TiO_2 photocatalytic technique for indoor air purification.

Keywords: Air purification; Formaldehyde; TiO_2 hydrosol; Photocatalytic activity

1. Introduction

Indoor air quality (IAQ) within buildings has been paid great attention, since many metropolitan generally spend more than 80% of time in an indoor environment. The sick building syndrome has been a critical concern, especially in some urban cities, such as Hong Kong, Guangzhou and Beijing of China [1,2]. Indoor air pollutants mainly include carbonyl compounds, nitrogen oxides (NO_x) and volatile organic compounds (VOCs), which can cause adverse health impacts on occupants [3]. These pollutants are emitted from different sources such as combustion by-products, cooking, construction materials, office equipment, consumer products, and nearby traffic vehicles. Formaldehyde (HCHO) is a representative carbonyl compound as one of the major indoor air pollutants, coming from the furnishings and decorating materials, and frequently causing cancer and other sickness. Formaldehyde pollution has received much attention from local people and government since the concentration of indoor formaldehyde usually might be at ppbv to ppmv levels in China [4–6], which is much higher than the concentration of the WHO guideline (80 ppbv, or 0.1 mg m^{-3}). To improve IAQ, the abatement of formaldehyde has become the problem that should be urgently solved.

TiO_2 photocatalysis has become a promising technique for the degradation of aqueous or gaseous toxic organic pollutants for water and wastewater treatment, and air purification owing to its environmental benign [7–12]. TiO_2-based microsphere has been developed for the application for wastewater treat-

* Corresponding author. Tel.: +86 20 87024721; fax: +86 20 87024123.
E-mail address: cefbli@soil.gd.cn (F.-b. Li).

0304-3894/$ – see front matter © 2007 Elsevier B.V. All rights reserved.
doi:10.1016/j.jhazmat.2007.07.003

ment because it can be used repeatedly [13–15]. However, one of the difficulties in application of TiO_2 for indoor air purification is how to coat the catalysts such as P-25 powder onto walls, windows, or furniture easily and durably, without any significant blights such as changes in color and transparency of materials after coating. The precursor sols for conventional TiO_2 thin films should be first coated on the substrate, and then sintered at 400–500 °C to acquire higher crystalline because a good anatase structure is to need a higher sintering temperature more than 400 °C for a sol–gel process [16–18]. TiO_2 hydrosol would be a more suitable catalyst since it is easy to coat and form a stable TiO_2 thin film on the substrates at room temperature and harmless to the materials. The preparation of TiO_2 hydrosols has been reported by means of different chemical precipitation–peptization processes at low temperatures (<100 °C), in which titanium butoxide ($Ti(OBu)_4$) [19], titanium ethoxide ($Ti(OC_2H_5)_4$) [20], titanium tetraisopropoxide ($Ti(OC_3H_7)_4$) [21], and titanium tetrachloride ($TiCl_4$) [22] were used as precursors, and HNO_3, HCl, or tetraalkylammonium hydroxides (TANOHs) were as peptizating catalysts. However, these TiO_2 hydrosols contained a significant amount of organic impurities resulted from either the above-mentioned precursors or peptizating agents. To avoid any organic impurities in the product TiO_2 hydrosols, titanium tetrachloride ($TiCl_4$) could be used as a precursor, but the preparing condition needs to be carefully controlled due to its strong volatility.

The aim of our work in this study was to prepare some organic-free TiO_2 hydrosols with low costs, which are photocatalytically active, stable, and easy be coated on the substrates. Titanium sulfate ($TiOSO_4$) or metatitanic acid (H_2TiO_3) would be better precursors, since they have much lower volatility and costs than $TiCl_4$. In this study, two types of TiO_2 hydrosols were prepared with $TiOSO_4$ and H_2TiO_3, respectively by a chemical precipitation–peptization method at low temperature of 65 °C. The photocatalytic activity of them was evaluated for the degradation of formaldehyde in a gaseous phase under UVA illumination. Effects of various factors on the reaction rates were also studied to optimize the reaction conditions for practical applications.

2. Experimental

2.1. Materials

$TiOSO_4$ with analytical grade was obtained from Shanghai Chemical Ltd., and H_2TiO_3 was purchased from Panzhihua Iron & Steel Research Institute, China. NH_4OH, HNO_3, and other chemicals with analytical grade were obtained from Shanghai Reagent Ltd. The deionized water was prepared by a RO purification system. Degussa P-25 with 80% anatase and 20% rutile was obtained from Degussa AG Company in Germany.

2.2. Preparation of TiO_2 hydrosols

TiO_2 hydrosols were prepared by a hydrothermal process using either $TiOSO_4$ or H_2TiO_3 as a precursor with the following procedure: 120 g of $TiOSO_4$ or 100 g of H_2TiO_3 was added into 2 l of water to get a solution or suspension after stirring continuously for 1 h. Then, the ammonia was dropped into the solution very slowly until pH was increased to above 9. The resulting suspension was stirred continuously for 3 h, and then filtered. The filter cake produced from both $TiOSO_4$ and H_2TiO_3 was washed with the deionized water repeatedly for several times until no sulfate ion was present (determined by 0.5 M barium chloride solution), and pH value was at 7.0. In this way, impurities could be substantively removed. Finally, the filter cake was mixed with the deionized water to form uniform suspension. 200 ml of nitric acid with a concentration of 10% (v/v) was dropped therein to adjust the pH value to be between 1 and 2. The resulting suspension was stirred continuously at room temperature for 4 h, followed by stirring and heating at a temperature of 65 °C. The suspension was peptized for 24 h, and then TiO_2(anatase) hydrosol was obtained, named as TOSO or HTO.

2.3. Characterization of TiO_2 hydrosols

To characterize the properties of the prepared TiO_2 hydrosols, the titania xerogel powder was prepared through gelation treatment at 65 °C for 24 h. The X-ray powder diffraction (XRD) patterns were recorded on a Rigaku D/Max-III A diffractometer at room temperature, operating at 30 kV and 30 mA, using a Cu Kα radiation (λ = 0.15418 nm). The phases were identified by comparing diffraction patterns with those on the standard powder XRD cards compiled by the Joint Committee on Powder Diffraction Standards (JCPDS). The crystal sizes were calculated by Scherrer's formula [12,23]. If the sample contains anatase and brookite phases, the mass fraction of brookite can be calculated according to Eq. (1), where A_A and A_B represent the integrated intensities of the anatase (1 0 1) and brookite (1 2 1) peaks, respectively [23].

$$W_B = \frac{2.721A_B}{0.886A_A + 2.721A_B} \quad (1)$$

The specific surface area (S_{BET}) and total pore volume were measured by the Brunauer–Emmett–Teller (BET) method, in which the N_2 adsorption at 77 K using an ASAP 2020 Sorptometer was applied. The prepared xerogel sample was degassed at 90 °C prior to nitrogen adsorption measurements. The pore size distribution was determined by the Barret–Joyner–Halender (BJH) method according to their desorption isotherm [24]. The nitrogen adsorption volume at the relative pressure (P/P_0) of 0.9733 was used to determine the pore volume and average pore sizes. The surface morphology of the catalysts was observed using scanning electron microscopy (SEM Leica Stereoscan 400i series). Fourier transform infrared (FTIR) spectra were recorded with a FTIR spectrometer (model Vector 33, Bruker Co.) at room temperature. The particle size distributions (PSD) of the hydrosols were directly determined by a light-scattering size analyzer (Beckman N5, USA). The UV–vis absorption spectra and transmittance spectra of the hydrosols in the wavelength range of 200–600 nm were obtained using a TU-1801 UV–vis spectrophotometer (Beijing, China).

2.4. Photodegradation of formaldehyde

Formaldehyde was selected a model pollutant to evaluate the photocatalytic activity of the prepared TiO_2 hydrosols. The experiments of gaseous formaldehyde degradation were conducted in a 0.1 m^3 photoreactor made of stainless steel. The reactor was placed in a small room where temperature and humidity were well controlled. P-25 was usually used as a control for evaluating the photocatalytic activity of the prepared samples for indoor air purification [25–29]. In this experiment, TiO_2 hydrosol or P-25 suspension was sprayed onto a piece of glass with a total area of 0.05 m^2 (25 cm × 20 cm). The TiO_2-coated glass sheet was dried in an oven at 65 °C for about 12 h to evaporate the adsorbed water and then cooled down to room temperature before use. The TiO_2-coated glass sheet film was fixed inside the reactor, and a set of 8-W Philip UV lamps with the main emission peak at 365 nm was placed at 2 cm above the glass sheet (I = 1.42 mW cm^{-2}). Then, a certain amount of formaldehyde gas was purged into the photoreactor from the standard gaseous formaldehyde cylinder (Foshan, China). The formaldehyde was allowed to reach adsorption/desorption equilibrium on the surface of catalyst in the reactor for 2 h prior to UV light irradiation. All the experiments were carried out at 25 ± 1 °C. The humidity was controlled with a humidifier (including two parts: one was used to produce dry air and the other was used for wet air) before photoreaction. The analysis of formaldehyde in the reactor was conducted with a formaldehyde monitor (Interscan 4160, USA). Each experiment lasted for 3 h. To analyze kinetically this experimental data of the HCHO decomposition, we introduced the Langmuir–Hinshelwood equation, in which the reaction rate (r) varies with the proportionally surface coverage (θ) as

$$r = k\theta = \frac{kKC}{1 + KC} \quad (2)$$

where k and K are the reaction rate constant and the adsorption equilibrium constants, and C is the concentration of HCHO. Owing to the complex mechanism of reactions, it is difficult to develop a model for the dependence of the photocatalytic degradation rate on the experimental parameters for the whole treatment time. Thus, kinetic modeling of the photocatalytic process is usually restricted to the analysis of the initial rate of photocatalytic degradation. This can be obtained from the initial slope and the initial HCHO concentration in an experiment in which the variation of the HCHO concentration is measured as a function of time. The extrapolation of the photocatalytic degradation rate to time = 0 avoids the possible interference from by-products. The measurements were repeated for each catalytic system, and the experimental error was found to be within ±5%.

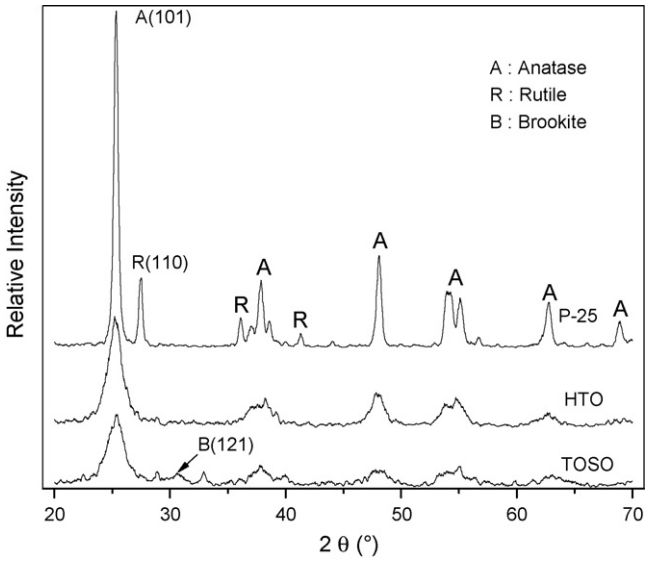

Fig. 1. X-ray diffraction patterns (XRD) of P-25 powder, HTO and TOSO sol particles.

3. Results and discussion

3.1. XRD analyses

The crystal structure of TiO_2 hydrosol xerogel powders (TOSO and HTO) was examined by XRD and the results are presented in Fig. 1 and Table 1, respectively. The XRD patterns showed that HTO sample had a pure anatase structure, and TOSO had mainly anatase structure with a weak brookite peak at $2\theta = 31^\circ$ (about 4%), while P-25 powder had a mixed crystal structure of anatase (about 80%) and rutile phase (about 20%). It was found that while the crystalline of HTO was higher than that of TOSO from the intensity of their (1 0 1) peak, the crystalline of P-25 was significantly higher than both of TOSO and HTO. The crystal sizes of TOSO and HTO were estimated by the Scherrer equation to be 5.6 and 11.3 nm, respectively, much less than that of P-25 (35.1 nm).

Table 1
the characteristic of HTO, TSO and P-25 powder

Sample	Crystal structure[a]	Crystal size (nm)[b]	Particle size (nm)[c]	Surface area (m^2/g)[d]	Pore volume (cm^3/g)[e]	Pore size (nm)[e]
HTO	A	11.3	24.2	379.0	0.499	5.3
TOSO	A + B (4%)	5.6	6.4	343.8	0.207	2.7
P-25 [23]	A + R (20%)	35.1	174	63.0	0.060	–

[a] A, B and R denote anatase, brookite and rutile, respectively.
[b] Crystal size of TiO_2 was determined by XRD using Scherrer equation.
[c] Average particle size was determined by PSD.
[d] The BET surface area was determined by multipoint BET method using the adsorption data.
[e] Pore volume and average pore size were determined by nitrogen adsorption at the relative pressure (P/P_0) of 0.9733.

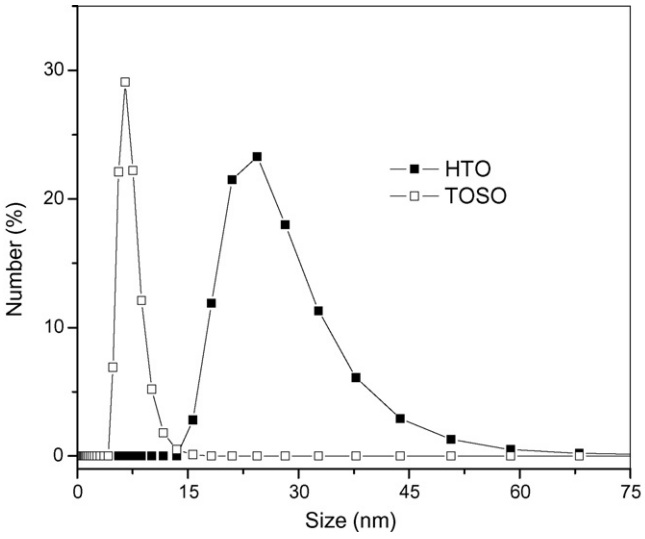

Fig. 2. Particle size distributions (PSD) of TOSO and HTO.

3.2. PSD, morphology and BET–BJH analyses

The PSD is an important parameter to show the property about the stability and transparence of the hydrosols. As shown in Fig. 2, the PSD results demonstrated that both the HTO and TOSO samples had a single-modal distribution characteristic with smaller particle sizes and more uniform PSD than P-25. The PSD of HTO and TOSO was in the range of 12.8–55.7 and 4.2–13.5 nm, respectively, both of which were far less than that of P-25 in the range of 148–208 nm [30]. The particle sizes of TiO_2 hydrosols determined by the PSD method were in good agreement with the crystal size determined by XRD. For example, the average particle size of TOSO (6.4 nm) was very close to its crystal size (5.6 nm), indicating an almost complete mono-dispersed hydrosol, while the average particle size of HTO (24.2 nm) was slightly larger than its crystal size (11.3 nm), due to the slight aggregation. Furthermore, it was clear that the average particle size of P-25 was much larger than its crystal size, probably due to the severe aggregation during its calcinations process.

SEM images (Fig. 3) showed the morphology of the hydrosol xerogel powders obtained from HTO and TOSO. It was shown in Fig. 3(a) that HTO particles could be seen clearly and showed a mixed structure of micropores and mesopores together. Additionally, there were some aggregates, which were probably caused restructuring of TiO_2 by the phase transformation from amorphous to anatase. Conversely, TOSO particles and porous structure presented in Fig. 3(b) were not very clear. It could be seen that the powders were heavily aggregated with some bulk aggregates of amorphous and microcrystalline appearance, resulting in a small amount of pores. It was because the hydrosols had to be prepared through gelation treatment before the SEM measurements, resulting in the severe aggregates.

To investigate the pore size distribution and adsorption properties of TiO_2 hydrosols, N_2 adsorption/desorption isothermal tests were carried out by the BET–BJH method, and their isotherm curves are presented in Fig. 4. The isotherm curves

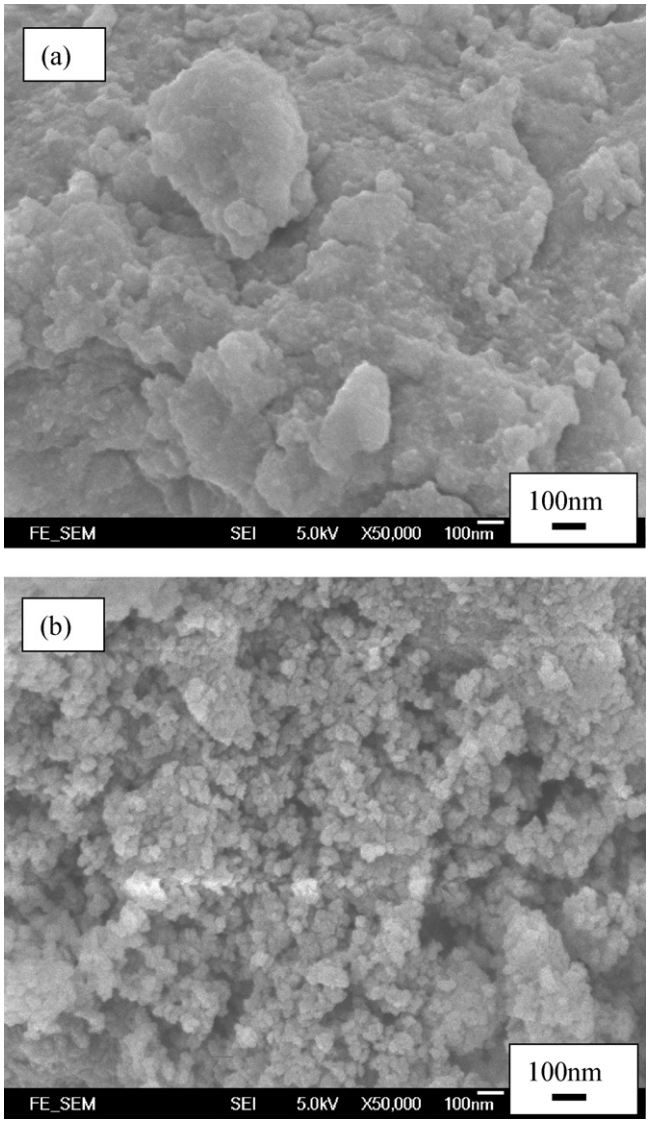

Fig. 3. Scanning electron microscopy (SEM) of (a) HTO and (b) TOSO sol particles.

for both HTO and TOSO (Fig. 4(a)) showed the Type IV curves. Their narrow hysteresis loops exhibited a typical pattern of Type II at a relative pressure from 0.4 to 0.6 (TOSO) and 0.6 to 0.9 (HTO), indicating that these catalysts might have porous structures. The corresponding pore size distributions are shown in Fig. 4(b). It can be seen that the pore size of TOSO was dominantly distributed between 1.80 and 4.21 nm with a peak value at 3.40 nm while that of HTO was mainly distributed between 4 and 13 nm with a peak value at 7.37 nm. The average pore sizes were calculated on the basis of pore size distribution data to be 2.7 nm for TOSO and 5.3 nm for HTO (Table 1). In the meantime, the surface areas and average pore sizes of hydrosols were determined by the BET method and are listed in Table 1. HTO and TOSO had the surface areas of 379.0 and 323.8 $m^2\,g^{-1}$, significantly larger than that of P-25 powder (63 $m^2\,g^{-1}$). Moreover, the pore volumes of HTO and TOSO were determined to be 0.499 $cm^3\,g^{-1}$ and 0.207 $cm^3\,g^{-1}$, respectively. It can be noted that the smaller particle size of TOSO may not lead to the larger

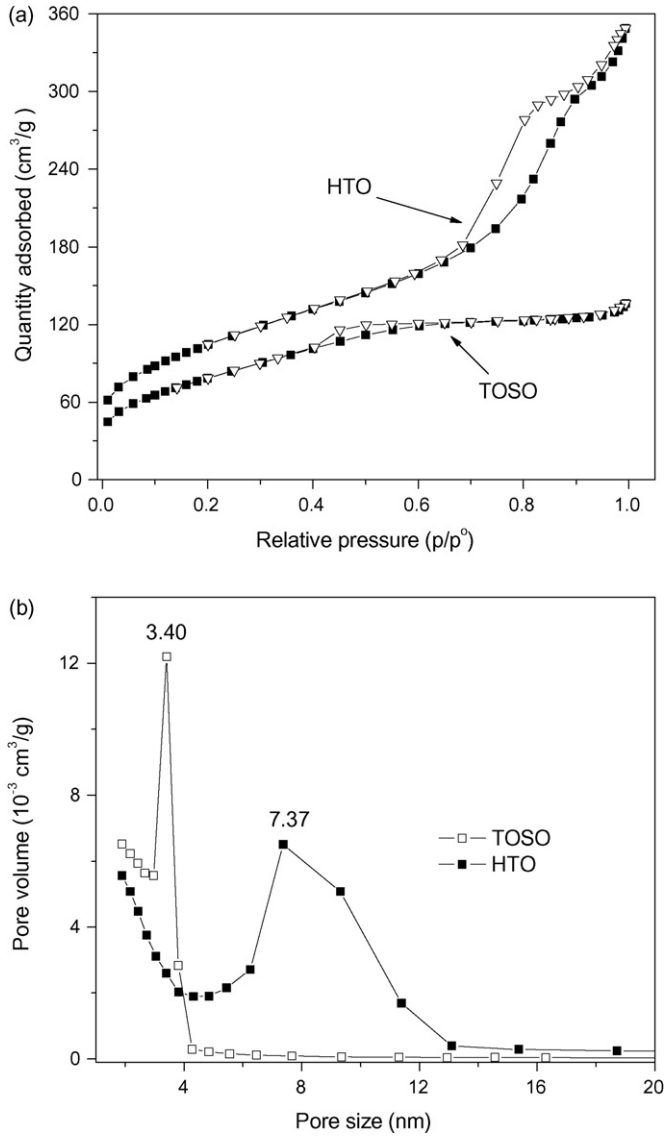

Fig. 4. N_2 adsorption–desorption isotherms of (a) HTO and TOSO sol particles and (b) pore size distributions of TOSO and HTO sol particles.

surface area, compared to HTO, as a large amount of amorphous TiO_2 in TOSO may cover the pores and reduce the total surface areas.

3.3. UV–vis transmittance spectra and absorption spectra

To determine the transparency of aqueous TiO_2 solution, three solutions/suspension containing TOSO, HTO or P-25 with the same solid content of 0.050 wt% were prepared, respectively. The UV–vis transmittance spectra of three samples were examined and are shown in Fig. 5. It is clear that the transparence can be ranked in an order of TOSO > HTO ≫ P-25, which confirmed that the aqueous hydrosol solution had much higher transparency than the aqueous TiO_2 powder suspension. Furthermore, the UV–vis absorption spectra of TiO_2 hydrosols were also studied (not shown here). The results showed that both HTO and TOSO hydrosols did not demonstrate any optical absorption in the visible region (wavelength > 400 nm). Moreover, the transparency of TOSO was higher than that of HTO due to the smaller particle sizes according to Table 1 and PSD results.

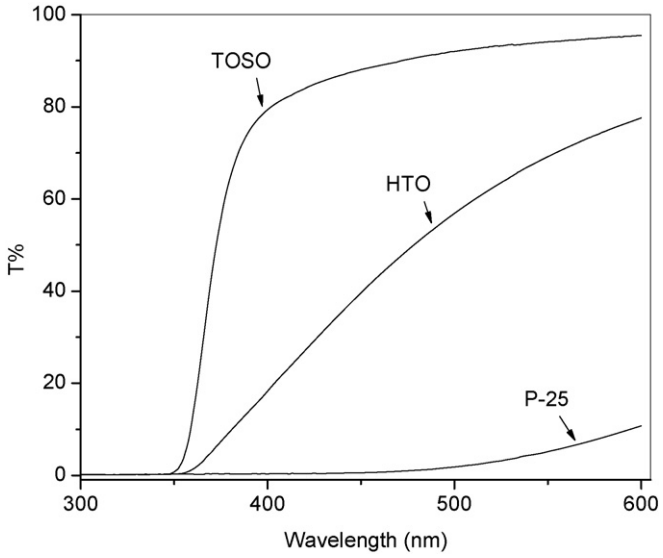

Fig. 5. UV–vis transmittance spectra of TOSO, HTO and P-25 suspension.

3.4. FTIR analyses

The FTIR transmittance spectra of P-25 powder and the xerogel powder of TiO_2 hydrosol were determined by the KBr pellets method and are presented in Fig. 6. A narrow absorption band at 1385 cm^{-1} attributing to the coexisted NO_3^- groups resulted from the HNO_3 used in the peptization process. A wide absorption band between 400 and 750 cm^{-1} was corresponded to Ti–O in the xerogel powder. Some broader peaks at 3000–3500 cm^{-1} and a strong peak at 1634 cm^{-1} were attributable to the O–H stretching vibration of water, Ti–OH group, and hydrated species on the TiO_2 surface, respectively. The difference in peak intensity demonstrated that TiO_2

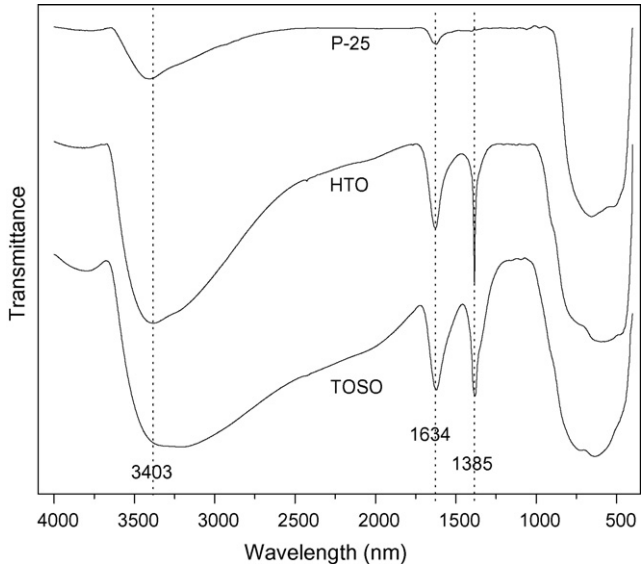

Fig. 6. FTIR transmittance spectrum of HTO and TOSO sol particles.

sol particles had more sufficient hydroxyl groups than P-25.

3.5. Photocatalytic activity for formaldehyde degradation

To investigate the photocatalytic activity of different catalysts, a set of gaseous experiments was carried out at the temperature of $25 \pm 1\,^{\circ}C$ and humidity of $50 \pm 1\%$. The catalyst was first coated on a piece of glass (25 cm × 20 cm) with the loading of $2\,mg\,cm^{-2}$. The initial formaldehyde concentration after injection was at 6.0 ± 0.2 ppmv, and it would be kept at 5.5 ± 0.2 ppmv after adsorption/desorption equilibrium. The removal percentage of formaldehyde after 3 h photoreaction was achieved by 76.9%, 82.4%, and 62.0% using TOSO, HTO, and P-25, respectively. The reaction rates (r) were determined to be 2.89, 3.31, and $1.92\,ppmv\,h^{-1}$ for TOSO, HTO, and P-25, respectively as shown in Fig. 7. It can be concluded that the reaction rates of formaldehyde degradation were ranked in an order of HTO > TOSO > P-25.

It was generally believed that the photocatalytic activity of TiO_2 should be a function of crystal structure, particle size, surface area and pore volume. The higher crystallinity and smaller particle size could have the higher photoactivity while the larger surface area and pore volume could have the higher adsorption capacity [23]. For the same degree of porosity, smaller grain sizes favor better intergranular charge-transfer, by promoting a greater intergranular contact surface, but also enhance the predominance of surface charge–carrier recombination over volume recombination, owing to a smaller volume and greater surface area. In this study, although TOSO and HTO had the lower crystallinity than P-25, the smaller particle size, much larger surface area and pore volume (as listed in Table 1) could enhance the efficiency of electron–hole separation and adsorption capacity, respectively. On the other hand, a greater amount of amorphous matter on the crystal surface, i.e., a weaker crystalline fraction, increases the surface recombination probability by inducing more surface defects that play a role of recombination centers. Despite the smallest particle size, TOSO had slightly lower photoactivity than HTO due to its higher amount of amorphous matter.

3.6. Effects of various factors on the formaldehyde degradation

The HTO hydrosol was used to study the effects of various factors on the formaldehyde degradation, due to its higher photoactivity and stable properties.

3.6.1. Effect of the TiO_2 amount

In photocatalytic degradation of organic compounds, the optimal TiO_2 concentration depends mainly on both the nature of the compounds and the reactor geometry [31–33]. In this work, the influence of TiO_2 amount on HCHO photodegradation was investigated on a piece of square glass (25 cm × 20 cm). A set of gaseous experiments with the TiO_2 solid loading from 0 to $4\,mg\,cm^{-2}$ was carried out at the humidity of $50 \pm 1\%$ and the initial HCHO concentration 5.5 ± 0.2 ppmv after adsorption/desorption equilibrium for 3 h. The reaction rates (r) for different TiO_2 loadings are presented in Fig. 8. These experiments demonstrated that the photocatalytic reaction rates did not increase significantly when the TiO_2 loading was more than $2\,mg\,cm^{-2}$ under this experimental condition.

3.6.2. Effect of initial HCHO concentration

To study the kinetics of the photocatalytic reaction of HCHO, a second set of experiments using a catalyst loading of $2\,mg\,cm^{-2}$ under a humidity of $50 \pm 1\%$ at room temperature was performed with different initial HCHO concentration in the range of 0.8–5.3 ppmv. Fig. 9 represented the reaction rates (r) for the HCHO decomposition at different initial concentrations. It was clear that the rate of HCHO decomposition is relatively high in the region of high HCHO concentration, but it is quickly

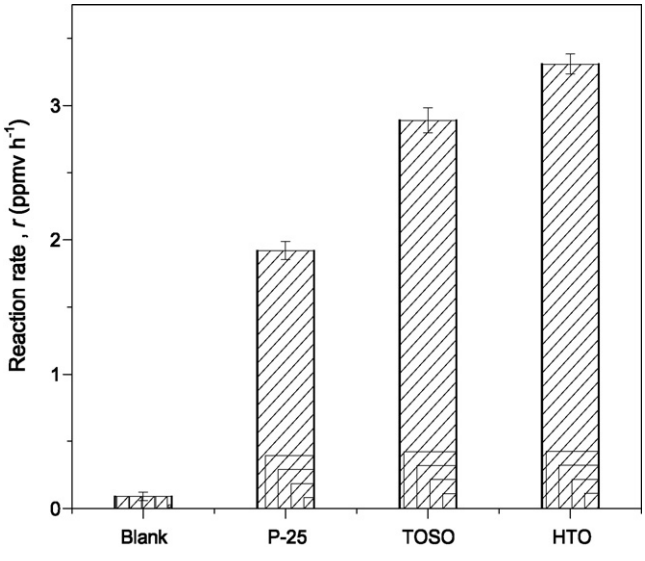

Fig. 7. Photocatalytic activity and the reaction rates (r) of HTO, TOSO and P-25 for formaldehyde degradation: humidity $50 \pm 1\%$, catalyst loading $2\,mg\,cm^{-2}$, initial HCHO concentration 5.5 ± 0.2 ppmv.

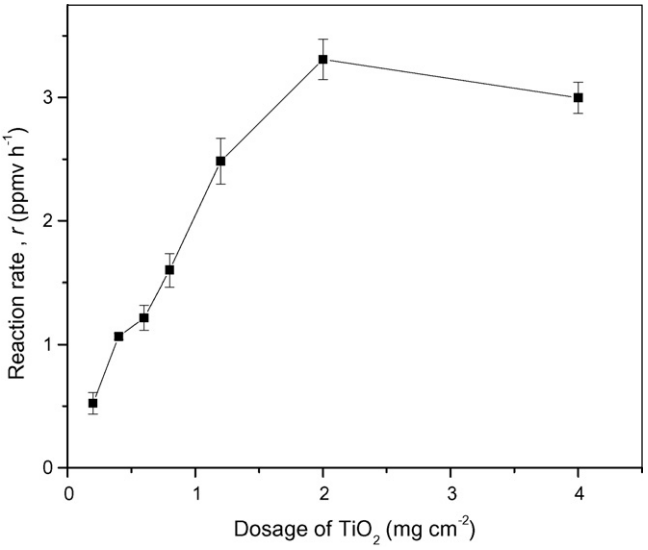

Fig. 8. The reaction rates (r) of formaldehyde degradation with different amount of HTO catalyst: humidity $50 \pm 1\%$, initial HCHO concentration 5.5 ± 0.2 ppmv.

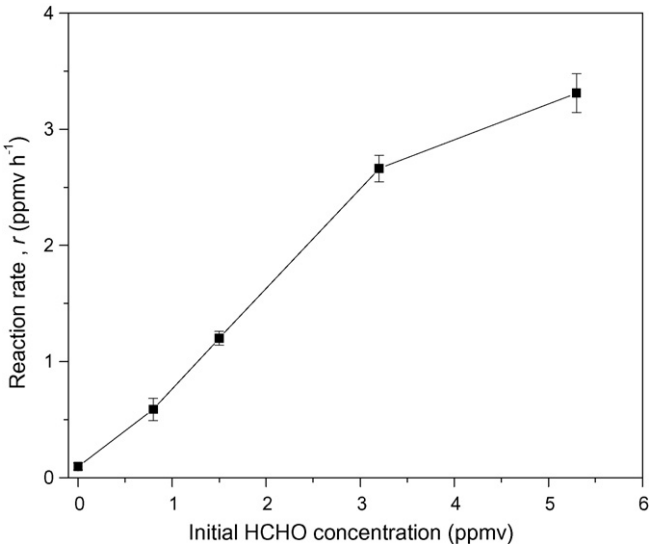

Fig. 9. The reaction rates (r) of photodegradation under different initial formaldehyde concentration: humidity $50 \pm 1\%$, HTO catalyst loading $2\,mg\,cm^{-2}$.

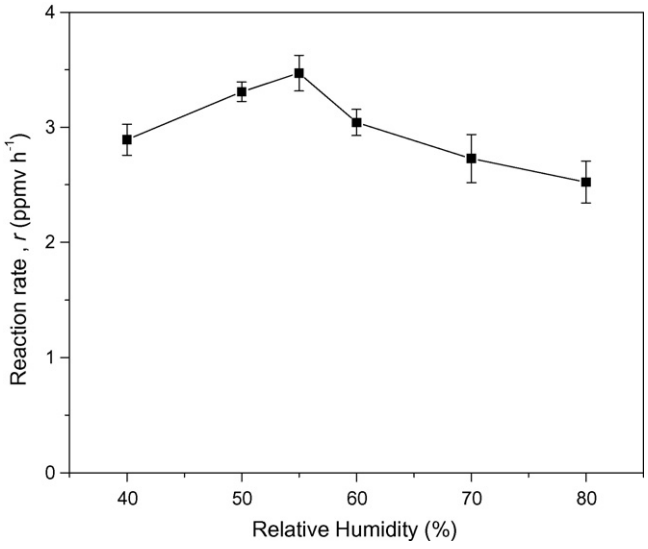

Fig. 10. The reaction rates (r) of formaldehyde degradation under different relative humidity (RH): HTO catalyst loading $2\,mg\,cm^{-2}$ and initial HCHO concentration 5.5 ± 0.2 ppmv.

slowed down in the region of low HCHO concentration. For example, the rate of HCHO decomposition at the initial concentration of 5.3 ppmv was 3.31 ppmv h^{-1}, more than five times of that at the initial concentration of 0.8 ppmv (0.588 ppmv h^{-1}). In this gas-phase photooxidation, the static photocatalytic rate is maybe affected by collision frequency. Only when the formaldehyde molecule reaches to the catalyst surface the photooxidation can occur. It is difficult for low concentration formaldehyde to be adsorbed on the photocatalytic surface, resulting photooxidation of low concentration formaldehyde costs long time [34–37].

3.6.3. Effect of relative humidity (RH)

To study the effect of relative humidity on HCHO removal, the third set of experiments with the initial HCHO concentration of 5.5 ± 0.2 ppmv and the TiO_2 loading of $2\,mg\,cm^{-2}$ was carried out under various relative humidity in the range of 40–80%. Fig. 10 presented the experimental results for the degradation of HCHO at different relative humidity. The results demonstrated that the optimal relative humidity was found to be 55% to achieve the highest reaction rate (3.47 ppmv h^{-1}). On one hand, the enhancement of photocatalytic reaction rate is frequently found in the presence of water vapor because hydroxyl groups or water molecules can behave as hole traps to form surface-adsorbed hydroxyl radicals [40,41]. The continuous consumption of hydroxyl radicals requires replenishment to maintain photocatalytic activity, only when there is a suitable equilibrium between consumption and adsorption. Hence, the lower relative humidity might result in a gradual decrease of surface-adsorbed hydroxyl radicals, thus inhibiting the removal of HCHO. On the other hand, moisture can be also detrimental to the photodegradation of the target organics [41–43]. The higher relative humidity might lead to competitive adsorption between H_2O and HCHO on the TiO_2 surface [33,38,39]. In addition, excess water might provide recombination centers for electron–hole pairs, which would result in a lower photocatalytic activity in the system. Therefore, the removal of HCHO increased with increased relative humidity in the lower range, but decreased with increased relative humidity in the higher range. It was found that the relative humidity of 55% was an optimal level for the removal of HCHO in gas phase.

3.7. The stability measurements

To elucidate the catalyst stability, the HTO and P-25 samples after photocatalytic reaction under UVA irradiation were characterized by XRD and FTIR. The XRD patterns (not shown here) of HTO and P-25 powders after HCHO degradation under UV irradiation exhibited almost the same phase and crystallinity as the fresh catalysts. Also, there was no significant difference between the fresh and used HTO samples in the FTIR transmittance spectra (Fig. 11). Because formic acid (HCOOH) as a main intermediate of formaldehyde photodecomposition was rapidly converted to CO_2 and H_2O, they did not accumulate on the TiO_2 catalysts [44]. However, some new peaks appeared at 1385 and 1690 cm^{-1} for the used P-25 sample, which could be assigned to a little of residual formic acid on the catalyst surface.

To further study the photoactivity stability of HTO for HCHO removal, the last set of experiments was carried out with the initial HCHO concentration of 5.5 ± 0.2 ppmv and the TiO_2 loading of $2\,mg\,cm^{-2}$ under relative humidity 55%. This was verified by a repeated experiment shown in Fig. 12. During six consecutive runs, the rate of HCHO degradation decreased slightly compared to that in the first run, with r equal to 3.47, 3.13, 3.24, 3.12, 3.22, and 3.01 ppmv h^{-1}, respectively. This decrease in the reaction rates was in agreement with the catalyst capacity toward HCHO adsorption, which also decreased. Both the decreases in the HCHO adsorption and in the HCHO degradation were mainly attributed to the intermediate competition with HCHO for the adsorptive sites. Although the reaction intermediates (formic acid) adsorbed on the catalyst from FTIR

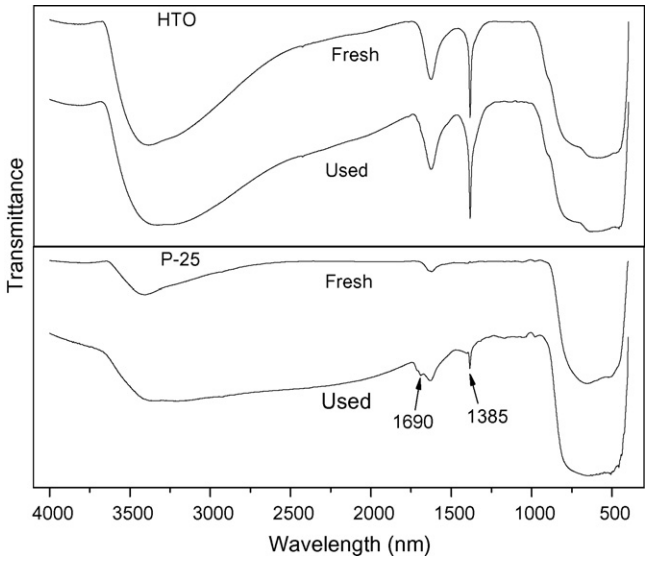

Fig. 11. FTIR transmittance spectrum of fresh and used catalyst: HTO and P-25.

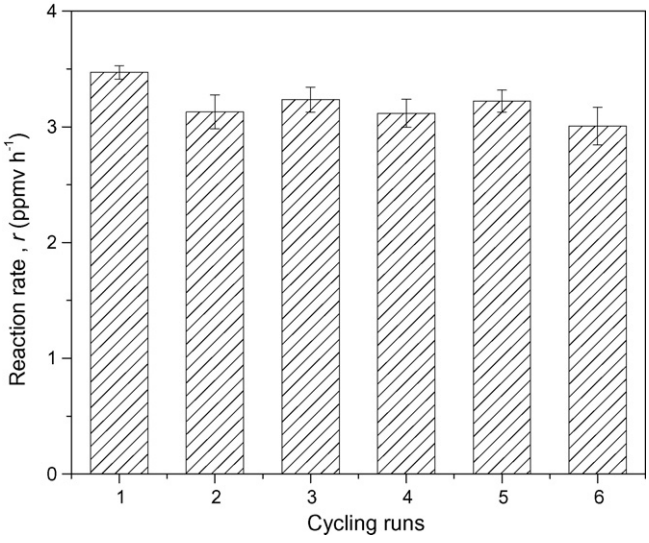

Fig. 12. The reaction rates (r) of cycling runs in formaldehyde photodegradation by the HTO catalyst under UVA irradiation: humidity $55 \pm 1\%$, catalyst loading $2\ mg\ cm^{-2}$, initial HCHO concentration 5.5 ± 0.2 ppmv.

results, they could be finally oxidized into CO_2 over the catalyst in situ under UVA irradiation. Therefore, after the six runs the photoreaction was still efficient. The repeated experiment showed that the HTO catalyst was reasonably stable and could be repeatedly used for the HCHO oxidation under UVA irradiation.

4. Conclusion

Two types of TiO_2 hydrosols were successfully prepared from $TiOSO_4$ and H_2TiO_3 by means of chemical precipitation–peptization method, respectively. These TiO_2 hydrosols compared with P-25 had smaller particle sizes, narrower particle size distributions, larger surface areas and pore volumes, and better transparency. The photocatalytic activity of the TiO_2 hydrosols for formaldehyde degradation can be ranked as an order of HTO > TOSO > P-25. Effects of various factors on the rates of HCHO degradation by HTO were studied. The reaction rates (r) increased with the amount of catalyst, and they did not increase significantly when the TiO_2 loading was more than $2\ mg\ cm^{-2}$. The rate constant of HCHO decomposition was relatively high in the region of high HCHO concentration, but it is quickly slowed down in the region of low HCHO concentration. The optimal humidity was 55% with the highest rate constant between 40 and 80%. Under these optimized conditions, the repeated experiment indicated the HTO catalyst was reasonably stable and could be repeatedly used for the HCHO oxidation under UVA irradiation. This study would be helpful to promote the industrialization and application of TiO_2 photocatalytic technique for indoor air purification.

Acknowledgements

The authors are thankful to the RGC grant of Hong Kong Government (RGC Grant No. PolyU5226/06E), National Natural Scientific Foundation of China (Nos. 20203007 and 20377011) and Guangdong Innovative Technique Foundation (2005B10301001) for financial supports to this work.

References

[1] K.F. Ho, S.C. Lee, P.K.K. Louie, S.C. Zou, Seasonal variation of carbonyl compound concentrations in urban area of Hong Kong, Atmos. Environ. 36 (2002) 1259–1265.
[2] J. Zhang, W. Hu, F. Wei, G. Wu, L. Korn, R.S. Chapman, Children's respiratory morbidity prevalence in relation to air pollution in four Chinese cities, Environ. Health Perspect. 100 (2002) 961–967.
[3] R. Atkinson, Atmospheric chemistry of VOCs and NOx, Atmos. Environ. 34 (2000) 2063–2101.
[4] Y. Feng, S. Wen, X. Wang, G. Sheng, Q. He, J. Tang, J. Fu, Indoor and outdoor carbonyl compounds in the hotel ballrooms in Guangzhou, China, Atmos. Environ. 38 (2004) 103–112.
[5] Z. Wang, Z. Bai, H. Yu, J. Zhang, T. Zhu, Regulatory standards related to building energy conservation and indoor-air-quality during rapid urbanization in China, Energy Build. 36 (2004) 1299–1308.
[6] Y. Zhao, B. Chen, Y. Guo, F. Peng, J. Zhao, Indoor air environment of residential buildings in Dalian, China, Energy Buildings 36 (2004) 1235–1239.
[7] M.R. Hoffmann, S.T. Martin, W. Choi, B.W. Bahnemann, Environmental applications of semiconductor photocatalysis, Chem. Rev. 95 (1995) 69–96.
[8] P.V. Kamat, Photochemistry on nonreactive and reactive (semiconductor) surfaces, Chem. Rev. 93 (1993) 267–300.
[9] A. Fujishima, T.N. Rao, D.A. Tryk, Titanium dioxide photocatalysis, J. Photochem. Photobiol. C 1 (2001) 1–21.
[10] O. Carp, C.L. Huisman, A. Reller, Photoinduced reactivity of titanium dioxide, Prog. Solid State Chem. 32 (2004) 33–177.
[11] J.C. Yu, J.G. Yu, W.K. Ho, L.Z. Zhang, Preparation of highly photocatalytic active nano-sized TiO_2 particles via ultrasonic irradiation, Chem. Commun. 19 (2001) 1942–1943.
[12] J.G. Yu, J.C. Yu, B. Cheng, S.K. Hark, K. Iu, The effect of F-doping and temperature on the structural and textural evolution of mesoporous TiO_2 powders, J. Solid State Chem. 174 (2003) 372–380.
[13] X.Z. Li, H. Liu, L.F. Cheng, H.J. Tong, Photocatalytic oxidation using a new catalyst – TiO_2 microsphere – for water and wastewater treatment, Environ. Sci. Technol. 37 (2003) 3989–3994.
[14] H. Liu, X.Z. Li, Y.J. Leng, W.Z. Li, An alternative approach to ascertain the rate-determining steps of TiO_2 photoelectrocatalytic reaction by electrochemical impedance spectroscopy, J. Phys. Chem. B 107 (2003) 8988–8996.

[15] H. Liu, H.T. Ma, X.Z. Li, W.Z. Li, M. Wu, X.H. Bao, The enhancement of TiO_2 photocatalytic activity by hydrogen thermal treatment, Chemosphere 50 (2003) 39–46.
[16] N. Negishi, K. Takeuchi, Preparation of a transparent thin-film photocatalyst for elimination of VOC, Res. Chem. Intermed. 29 (2003) 861–879.
[17] J.M. Wuw, B. Huang, Enhanced ability of nanostructured titania film to assist photodegradation of Rhodamine B in water through natural aging, J. Am. Ceram. Soc. 90 (2007) 283–286.
[18] S. Park, E. DiMasi, Y. Kim, W. Han, P.M. Woodward, T. Vogt, The preparation and characterization of photocatalytically active TiO_2 thin films and nanoparticles using successive-ionic-layer-adsorption-and-reaction, Thin Solid Films 515 (2006) 1250–1254.
[19] J. Yang, S. Mei, J.M.F. Ferreira, In situ preparation of weakly flocculated aqueous anatase suspensions by a hydrothermal technique, J. Colloid Interf. Sci. 260 (2003) 82–88.
[20] J. Yang, S. Mei, J.M.F. Ferreira, Hydrothermal synthesis of TiO_2 nanopowders from tetraalkylammonium hydroxide peptized sols, Mater. Sci. Eng. C 15 (2001) 183–185.
[21] F. Cot, A. Larbot, G. Nabias, L. Cot, Preparation and characterization of colloidal solution derived crystallized titania powder, J. Eur. Ceram. Soc. 18 (1998) 2175–2181.
[22] D. Lee, T. Liu, Preparation of TiO_2 sol using $TiCl_4$ as a precursor, J. Sol–Gel Sci. Technol. 25 (2002) 121–136.
[23] J.G. Yu, M.H. Zhou, B. Cheng, H.G. Yu, X.J. Zhao, Ultrasonic preparation of mesoporous titanium dioxide nanocrystalline photocatalysts and evaluation of photocatalytic activity, J. Mol. Catal. A 227 (2005) 75–80.
[24] S.L. Gregg, K.S.W. Sing, Adsorption, Surface Area and Porosity, Academic Press, London, 1982.
[25] M. Keshmiri, T. Troczynski, M. Mohseni, Oxidation of gas phase trichloroethylene and toluene using composite sol–gel TiO_2 photocatalytic coatings, J. Hazard. Mater. B128 (2006) 130–137.
[26] M.H. Zhou, J.G. Yu, B. Cheng, Effects of Fe-doping on the photocatalytic activity of mesoporous TiO_2 powders prepared by an ultrasonic method, J. Hazard. Mater. B 137 (2006) 1838–1847.
[27] J.G. Yu, J.C. Yu, M.K.P. Leung, W.K. Ho, B. Cheng, X.J. Zhao, J.C. Zhao, Effects of acidic and basic hydrolysis catalysts on the photocatalytic activity and microstructures of bimodal mesoporous titania, J. Catal. 217 (2003) 69–78.
[28] C.H. Ao, S.C. Lee, J.C. Yu, Photocatalyst TiO_2 supported on glass fiber for indoor air purification: effect of NO on the photodegradation of CO and NO_2, J. Photochem. Photobiol. A 156 (2003) 171–177.
[29] W.H. Ching, M. Leung, D.Y.C. Leung, Solar photocatalytic degradation of gaseous formaldehyde by sol–gel TiO_2 thin film for enhancement of indoor air quality, Solar Energy 77 (2004) 129–135.
[30] Y.B. Xie, C.W. Yuan, Visible-light responsive cerium ion modified titania sol and nanocrystallites for X-3B dye photodegradation, Appl. Catal. B 46 (2003) 251–259.
[31] J. Giménez, D. Curcó, M.A. Queral, Photocatalytic treatment of phenol and 2,4-dichlorophenol in a solar plant in the way to scaling-up, Catal. Today 54 (1999) 229–243.
[32] F. Shiraishi, S. Yamaguchi, Y. Ohbuchi, A rapid treatment of formaldehyde in a highly tight room using a photocatalytic reactor combined with a continuous adsorption and desorption apparatus, Chem. Eng. Sci. 58 (2003) 929–934.
[33] H. Liu, Z. Lian, X. Ye, W. Shangguan, Kinetic analysis of photocatalytic oxidation of gas-phase formaldehyde over titanium dioxide, Chemosphere 60 (2005) 630–635.
[34] P. Chin, L.P. Yang, D.F. Ollis, Formaldehyde removal from air via a rotating adsorbent combined with a photocatalyst reactor: kinetic modeling, J. Catal. 237 (2006) 29–37.
[35] T.N. Obee, R.T. Brown, TiO_2 photocatalysis for indoor air applications: effects of humidity and trace contaminant levels on the oxidation rates of formaldehyde, toluene, and 1,3-butadiene, Environ. Sci. Technol. 29 (1995) 1223–1231.
[36] E. Obuchi, T. Sakamoto, K. Nakano, et al., Photocatalytic decomposition of acetaldehyde over TiO_2/SiO_2 catalyst, Chem. Eng. Sci. 54 (1999) 1525–1530.
[37] J.M. Coronado, M.E. Zorn, I. Tejedor-Tejedor, M.A. Anderson, Photocatalytic oxidation of ketones in the gas phase over TiO_2 thin films: a kinetic study on the influence of water vapor, Appl. Catal. B 43 (2003) 329–344.
[38] C.S. Turchi, D.F. Ollis, Photocatalytic degradation of organic-water contaminants—mechanisms involving hydroxyl radical attack, J. Catal. 122 (1990) 178–192.
[39] M. Primet, P. Pichat, M.V. Mathieu, Infrared study of surface of titanium dioxides. 1. Hydroxyl groups, J. Phys. Chem. 75 (1971) 1216–1220.
[40] W.A. Jacoby, D.M. Blake, R.D. Noble, C.A. Koval, Kinetics of the oxidation of trichloroethylene in air via heterogeneous photocatalysis, J. Catal. 157 (1995) 87–96.
[41] S.B. Kim, S.C. Hong, Kinetic study for photocatalytic degradation of volatile organic compounds in air using thin film TiO_2 photocatalyst, Appl. Catal. B 35 (2002) 305–315.
[42] L. Cao, G. Zi, S.L. Suib, T.N. Obee, S.O. Hay, J.D. Freihaut, Photocatalytic oxidation of toluene on nanoscale TiO_2 catalysts: studies of deactivation and regeneration, J. Catal. 196 (2000) 253–261.
[43] N.N. Lichtin, M. Avudaithai, TiO_2-photocatalyzed oxidative degradation of CH_3CN, CH_3OH, C_2HCl_3, and CH_2Cl_2 supplied as vapors and in aqueous solution under similar conditions, Environ. Sci. Technol. 30 (1996) 2014–2020.
[44] M.L. Sauer, D.F. Ollis, Photocatalyzed oxidation of ethanol and acetaldehyde in humidified air, J. Catal. 158 (1996) 570–582.